Development and comparison of novel bioluminescent mouse models of pancreatic neuroendocrine tumor metastasis

University of Iowa Neuroendocrine Tumor Program

University of Iowa Holden Comprehensive Cancer Center

Courtney A. Kaemmer[1], Shaikamjad Umesalma[1], Chandra K. Maharjan[1], Devon L. Moose[2], Goutham Narla[3], Sarah Bell[4], Gideon K.D. Zamba[4,8], Patrick Breheny[4,8], Benjamin W. Darbro[5,8], Andrew M. Bellizzi6[,8], Michael D. Henry[7,8], and Dawn E. Quelle[1,6,8]

Departments of [1]Neuroscience and Pharmacology; [2]Cancer Biology Graduate Program; [4]Department of Statistics; [5]Department of Pediatrics; [6]Department of Pathology; [7]Department of Molecular Physiology and Biophysics; [8]Holden Comprehensive Cancer Center, University of Iowa; [3]Department of Medicine, University of Michigan

University of Iowa Children's Hospital

SUPPORTED BY THE IOWA NEUROENDOCRINE TUMOR SPORE

Background

Introduction

Neuroendocrine Tumors (NETs)

- Clinically challenging malignancies
- Arise in diverse organs
- Grow slowly
- Largely unresponsive to traditional therapies
- Drug resistance is a major problem in advanced disease (metastases)

40% of PNET patients have distant metastatic disease (mainly in the liver) at diagnosis

- Current therapies fail to improve overall survival
- Little known about mechanisms driving NET metastasis
- Pre-clinical models of PNET metastasis are lacking and greatly needed

Bioluminescence Imaging (BLI)

- Noninvasive, real-time imaging of tumor progression in animals
- Via the process of light emission
- Developed two bioluminescent PNET cell lines (BON1.luc and Qgp1.luc)

NET Advances

Clinical Relevance

Mouse metastasis models that mimic the patient disease will provide a greatly needed platform to test clinically relevant drug therapies

A better understanding of genes and pathways driving PNET development will provide new biomarkers of metastasis and drug targets

Project Goal

To establish novel mouse models of NET metastasis for use in developing and testing novel therapeutic interventions.

Results

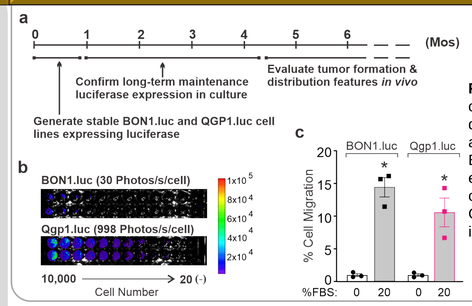

Figure 1. a) Timeline showing generation of luciferase-expressing cell lines *in vitro*, validation of maintained luciferase expression, and development of *in vivo* model involving monitoring of tumor formation and distribution. **b)** *In vitro* luciferase activity of serially diluted BON1.luc and Qgp1.luc cells, which were infected with retroviruses encoding luciferase plus neomycin resistance and stable polyclonal cell lines selected with G418. **c)** Relative migration of BON1.luc and Qgp1.luc cells induced with 20% FBS, normalized to samples plated in 0% FBS in a transwell migration assay.

Metastasis Models

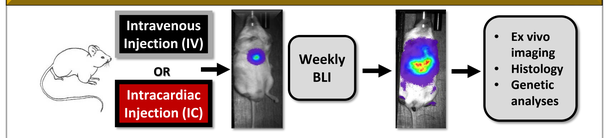

Figure 2: NSG mice were injected with two different luciferized PNET cell lines via intravenous (IV) or intracardiac (IC) routes. Mice were imaged weekly via bioluminescence imaging (BLI). Photos/sec were monitored to assess tumor location and burden. Mice were euthanized based on high BLI (photons/sec >10^9) or low Body Conditioning Score.

Intracardiac (IC) Mouse Model

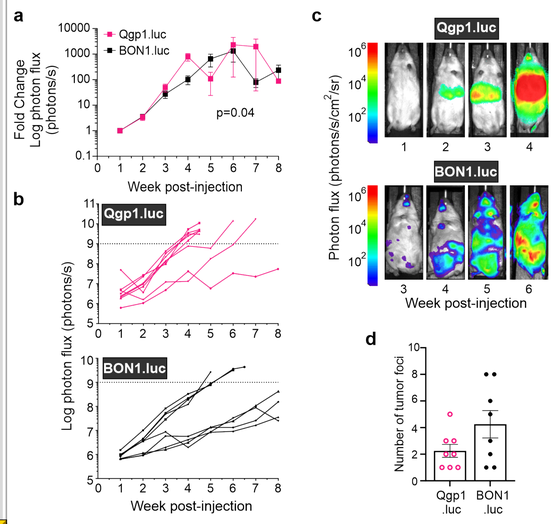

Figure 3 (Left). Intracardiac model of pNET metastasis. a) Average fold change from week one (mean +/- SEM) in Qgp1.luc and BON1.luc injected mice displayed in rest of the figure. **b)** Graphs of individual tumor growth rates in NSG mice (n = 8 per group), as measured by BLI, following intracardiac injection with Qgp1.luc (top) or BON1.luc (bottom) cells. Each line represents a single mouse with tumor growth quantified by total photon flux (photons per second) per animal over the indicated time. **c)** Longitudinal bioluminescence images at the indicated times (weeks) post-injection with Qgp1.luc (top) or BON1.luc (bottom) cells. Each set of images was taken from the same mouse. **d)** Number of tumor foci per mouse in BON1.luc versus Qgp1.luc animals based on quantified photon flux of tumors by ex vivo BLI. *, P<0.01 by Student's t-test.

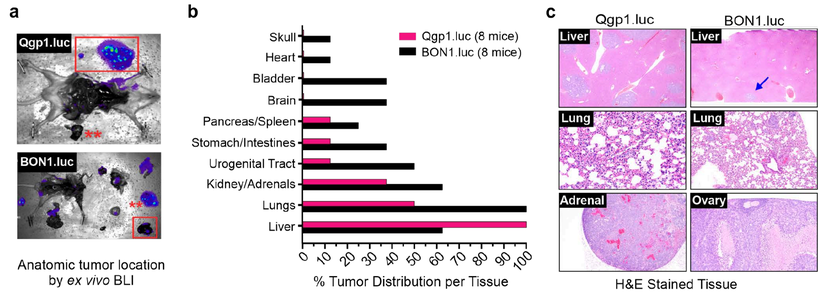

Figure 4 (Above). a) *Ex vivo* bioluminescent images (BLI) of tissues to pinpoint the different organ sites of tumor cell colonization. Red boxes, liver; red asterisk, lung. **b)** Quantified distribution of bioluminescent PNET cells per tissue. All BON1.luc-injected mice exhibited lung tumors while all QGP1.luc-injected mice exhibited liver tumors. **c)** H&E images of Qgp1.luc and BON1.luc tumors in the liver, lung, adrenal and ovary tissues, as indicated in the inset of each image.

Intravenous (IV) Mouse Model

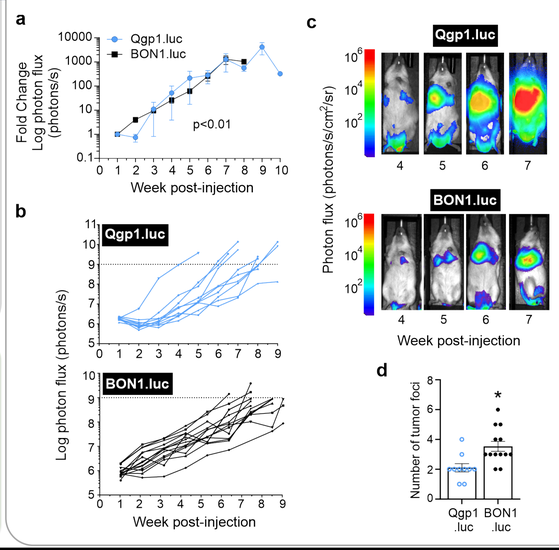

Figure 5 (Left). Intravenous model of pNET metastasis. a) Average fold change from week 1 (mean +/- SEM) in Qgp1.luc and BON1.luc injected mice. **b)** Graphs of individual tumor growth rates, as measured by BLI, in each NSG mouse following intravenous injection of Qgp1.luc cells (top, n=10 mice) and BON1.luc cells (bottom, n=13 mice). Each line reflects a single mouse with tumor growth quantified by total photon flux (photons per second) over the indicated time. **c)** Longitudinal bioluminescence images at the indicated times in weeks post-injection with Qgp1.luc (top) and BON1.luc (bottom) cells. Each set of images was taken from the same mouse. **d)** Number of tumor foci per mouse in Qgp1.luc and BON1.luc animals based on quantified photon flux of tumors by ex vivo BLI. *, P<0.05 by Student's t-test.

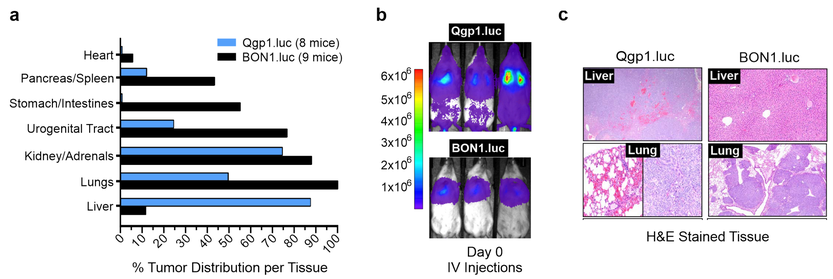

Figure 6 (Above). a) Quantification of the tissue distribution of bioluminescent PNET cells per indicated tissue. All BON1.luc-injected mice exhibited lung tumors and 87.5% Qgp1.luc-injected mice showed liver tumors. **b)** Day 0 IV injections imaged within 15mins showing successful IV injections. Qgp1.luc (3) female shown on top and BON1.luc (3) female shown on bottom **c)** H&E images from Qgp1.luc and BON1.luc tumors in the liver and lung as indicated in the inset of each image.

Conclusions

Table 1: Summary of BLI Model Findings

Tumors	Qgp1.luc		BON1.luc	
	IC	IV	IC	IV
#per mouse	2.3+/-0.49	2.1+/-0.28	4.3+/-1.03	3.5+/-0.33
Liver	100%	87.5%	62.5%	11.1%
Lungs	50%	50%	100%	100%
Kidney/Adrenals	37.5%	75%	62.5%	88.9%
Urogenital Tract	12.5%	25%	50%	77.8%
Stomach/Intestines	12.5%	0%	37.5%	55.6%
Pancreas/Spleen	12.5%	12.5%	25%	44.4%
Brain	0%	0%	37.5%	0%
Skull	0%	0%	12.5%	0%
Heart	0%	0%	0%	11.1%
Unknown	0%	12.5%	0%	22.2%

Table 1: BON1.luc cells show higher # tumor foci per mouse regardless of route of injection as they tend to colonize in a broad range of tissues. BON1.luc cells also show develop lung tumors in both models in 100% of mice. Qqp1.luc cells show a preference for liver metastasis regardless of route of injection.

Developed Novel PNET Metastasis Models

- Successfully developed 2 reliable methods for modeling NET metastatic colonization in mice.
- Tumor growth can be quantitatively tracked over time through non-invasive imaging, reducing the number of animals required.
- 100% tumor take from both IV (tail vein) and IC (intracardiac) administration.
- Qgp1.luc cells preferentially metastasized to the liver regardless of delivery route.
  - Unexpected and atypical for IV delivery of tumor cells
  - Exciting since the majority of patient PNETs metastasize to the liver.
- BON1.luc always formed tumors in the lung regardless of delivery route but also colonized a wider variety of tissues compared to Qgp1.luc, including liver, adrenal glands, kidney and ovaries with high frequency.
- Both models will enable rapid testing of innovative therapies with potential anti-metastatic activity.

Acknowledgements

This work was supported by NIH/NCI NET SPORE (P50 CA174521) and NCI core grant P30 CA086862 to the University of Iowa HCCC.